

# Copolymerization of Propylene with Poly(ethylene-*co*-propylene) Macromonomer and Branch Chain-Length Dependence of Rheological Properties

Edward Kolodka, Wen-Jun Wang, Shiping Zhu,\* and Archie E. Hamielec

Department of Chemical Engineering, McMaster University, 1280 Main Street West, Hamilton, Ontario L8S 4L7, Canada

Received July 22, 2002

**ABSTRACT:** A series of isotactic polypropylene (PP) samples with poly(ethylene-*co*-propylene) long chain branching were produced by a semibatch copolymerization of poly(ethylene-*co*-propylene) macromonomer (EPR), prepared in a high-temperature continuous stirred tank reactor (CSTR), and propylene using *rac*-dimethylsilylenebis(2-methylbenz[e]indenyl) zirconium dichloride/modified methylaluminoxane. The branch frequency and branch length of the copolymers were controlled by varying the stoichiometry and molecular weight of the EPR macromonomer, respectively. Long chain branch frequencies of up to 2.8 branches per chain were achieved, while the branch length was varied from 2500 to 17 000 g/mol. The effects of macromonomer concentration, macromonomer molecular weight, and reaction temperature on the copolymer chain properties were investigated. The rheological responses of the EPR-branched PP were determined. Branches below 7000 g/mol had little influence on the rheological behavior of the polymers. The zero shear viscosity, shear thinning property, and loss and storage moduli were found to be dependent on the branch length and branch frequency when the branch  $M_n$  was above 7000 g/mol. Elevated flow activation energies were observed with measured values of up to 51 kJ/mol. The physical and chemical properties of the copolymers were analyzed by gel permeation chromatography (GPC), FTIR, parallel-plate rheometry, and  $^{13}\text{C}$  NMR.

## Introduction

There has been considerable interest in the relationships between molecular architecture and viscoelastic behavior of polyolefins in recent years.<sup>1</sup> It has been demonstrated that the influence of long chain branching (LCB) on the thermorheological properties of polymers can be remarkable.<sup>2,3</sup> The precise effects of LCB are not well understood, however, because of the difficulty of producing well-defined samples with a broad range of molecular attributes.

There are many molecular properties that influence the physical characteristics of polymers including molecular weight (MW), molecular weight distribution (MWD), short chain branching (SCB), long chain branching (LCB), branch length, and branch frequency distribution. These properties act in concert, and separating individual influences has proven to be difficult. In an attempt to isolate the effect of branching from MW and MWD, there has been considerable interest paid to both linear and star-branched hydrogenated polybutadienes (HPB) synthesized via anionic polymerization.<sup>4–6</sup> This technique provides excellent control over the MW and MWD and has contributed fundamentally to the understanding of LCB. This technique, however, has only recently been applied to the study of comb-branched polymers.<sup>7</sup>

Recent innovations in single-site-type catalysts allow the production of model polymers with narrow molecular weight distributions (MWDs) and extremely narrow chemical composition distributions (CCDs).<sup>8,9</sup> Dow Chemical's constrained geometry catalyst (CGC) has been used to synthesize LCB polyethylenes of various

MWs and long chain branch densities (LCBD).<sup>10,11</sup> This catalyst, with its open configuration, produces long chain branching through the insertion of vinyl-terminated polyethylene (PE) formed in situ through  $\beta$ -hydride elimination or chain transfer to monomer. A precise control of the branch length is not possible using this technique. Recently, Shiono et al. and Weng et al. have demonstrated the ability of several innovative metallocene catalysts to incorporate previously produced macromonomers into growing polymer backbones, forming a comb structure.<sup>12–15</sup> This technique makes it possible to produce polymers with controlled branch density and branch length and with uniform backbones.

Extremely low levels of long chain branching have been shown to have significant influences on the viscoelastic behavior of polyolefins. Graessley et al.,<sup>4</sup> working with star-branched hydrogenated polybutadienes (HPB), observed significantly enhanced zero shear viscosities ( $\eta_0$ ) compared to linear polymers with similar molecular weights. It was demonstrated that the  $\eta_0$  of star-branched HPB varied exponentially with the arm molecular weight. Further studies by Jordan et al.<sup>16</sup> on asymmetric three-arm star HPB determined that the length necessary for a branch to behave as a long chain branch was  $2M_e$  ( $M_e$  = molecular weight between entanglements). It has been shown that  $M_e$  for PE is 1250. Yan et al.<sup>10</sup> observed significant enhancements in  $\eta_0$ , shear thinning, and flow activation energies in LCB PE produced in a continuous stirred tank reactor (CSTR) using CGC.

The temperature dependence of many polymers can be described using a time shift factor,  $a_T$ , as shown in eq 1.

$$\eta(T) = a_T(T)\eta(T_0) \quad (1)$$

where  $T_0$  is an arbitrary reference temperature. Poly-

\* To whom correspondence should be addressed. E-mail: zhuship@mcmaster.ca. Fax: (905) 521-1350. Phone: (905) 525-9140, ext 24962.

mers that behave in this manner are considered rheologically simple. Using the shift factor, one can construct a master curve from superimposed data generated at several temperatures. The temperature dependence of  $a_T$  for rheologically simple polymers, at temperatures well above the glass transition temperatures ( $T_g$ ), often follows an Arrhenius relation. The flow activation energy ( $E_a$ ), which is a measure of temperature sensitivity, is given by

$$a_T = \exp \left[ \frac{E_a}{R} \left( \frac{1}{T} - \frac{1}{T_0} \right) \right] \quad (2)$$

The viscoelastic behavior of several polymer types, including LCB PE, does not follow these simple relations and is considered to be rheologically complex. These polymers do not have a single activation energy but exhibit shear-dependent temperature sensitivity. At high shear rates, the loss modulus  $E_a$  is found to be approximately the same as a linear polymer and is dominated by the reptation of linear molecules.<sup>17</sup> However, at low shear rates, the  $E_a$  is significantly higher for long chain branched PE because of the cumulative effect of the relaxations of chains having various branch structures.<sup>18</sup>

In this paper, we describe the synthesis of comb-structured polypropylenes with isotactic polypropylene (PP) backbones and poly(ethylene-*co*-propylene) long chain branches. A series of branched polymers with controlled branch frequency and branch length were prepared. The branch length was varied from well below to well above  $M_c$  ( $M_c$  = critical entanglement length). The influences of the branch length and density on the shear viscosity and loss and storage moduli were then investigated. The shear-dependent activation energy was determined for all shear rates.

## Experimental Section

**Materials.** All manipulations involving air- and moisture-sensitive compounds were carried out under dry nitrogen in a glovebox. The catalyst *rac*-dimethylsilylenebis(2-methylbenz[e]indenyl) zirconium dichloride (MBI) was provided by Mitsubishi Chemicals. The constrained geometry catalyst,  $[C_5Me_4(SiMe_2N^iBu)]TiMe_2$  (CGC), and cocatalyst tris(pentafluorophenyl)boron (TPFPB) were provided by Dow Chemical as 10 and 3 wt % solutions in Isopar E. Modified methylaluminoxane (MMAO, 12 mol % of isobutylaluminoxane) was provided by Akzo as a 10 wt % solution in toluene. The catalysts and cocatalysts were used without further purification. Isopar E, used in the continuous stirred tank reactor (CSTR) for the macromonomer preparation, was purchased from Van Waters & Rogers Ltd. and dried over a mixture of 5A and 13X molecular sieves from Fisher Scientific and silica gel from Caledon Laboratories Ltd. The solvent was also deoxygenated by sparging with ultrahigh purity nitrogen (99.999%, Matheson Gas). Reagent-grade toluene for the semibatch reactor (SBR), provided by Caledon Laboratories, was refluxed over metallic sodium/benzophenone for 48 h and was distilled under a nitrogen atmosphere prior to use. Ethylene and propylene (polymerization grade, >99.5%) were purchased from Matheson Gas and further purified by passing through columns with CuO (Aldrich), Ascarite (Fisher Scientific), and molecular sieves (Grace-Davidson) to remove oxygen, carbon dioxide, and moisture, respectively. Polymer was treated with Irganox 1010 antioxidant to prevent degradation.

**Preparation of Macromonomer.** The poly(ethylene-*co*-propylene) (EPR) macromonomer samples were prepared in a 0.6 L high-temperature, high-pressure continuous stirred tank reactor (CSTR). The details regarding the reactor system and operation were reported in our previous work.<sup>19,20</sup> Polymeriza-

**Table 1. Reaction Conditions and Chain Properties of Poly(ethylene-*co*-propylene) Macromonomer Samples Prepared by High-Temperature Continuous Stirred Tank Reactor<sup>a</sup>**

macrom no.	$T$ , °C	$[E]_0$ , mol/L	$[P]_0$ , mol/L	$M_n$ , g/mol	$M_w/M_n$	$F_p$	vinyl concn, %	vinylidene concn, %
1	150	0.33	1.09	2560	2.6	0.57	36	42
2	140	0.31	1.13	3900	2.5	0.58	37	39
3	130	0.59	0.83	6010	2.5	0.42	40	43
4	150	0.08	0.13	7820	2.4	0.28	42	44
5	140	1.02	0.42	11 200	2.5	0.21	44	43
6	130	0.11	0.11	17 100	2.0	0.28	43	45

<sup>a</sup> Experimental conditions: catalyst = CGC; cocatalyst = TPF-PB; 2nd cocatalyst = MMAO; solvent = Isopar-E;  $[CGC] = 15 \mu M$ ;  $[TPFPB] = 3 \mu M$ ;  $[MMAO] = 150 \mu M$ ; mean residence time = 4 min; pressure =  $3.45 \times 10^3$  kPa. <sup>b</sup>  $F_p$  = propylene molar fraction in copolymer.

**Table 2. Experimental Conditions for the Copolymerization of Propylene with Poly(ethylene-*co*-propylene) Macromonomers in Semibatch Reactor<sup>a</sup>**

run	macrom no. <sup>b</sup>	load (g/L)	$T$ (°C)
1	1	20	30
2	2	20	30
3	3	20	30
4	4	26	30
5	5	25	30
6	6	17.5	30
7	1	0	30
8	1	5	30
9	1	10	30
10	1	15	30
11	6	5	30
12	6	10	30
13	1	20	40
14	1	20	50

<sup>a</sup> Catalyst = *rac*-dimethylsilylenebis(2-methylbenz[e]indenyl) zirconium dichloride; cocatalyst = modified methylaluminoxane; pressure = 12.5 psig; volume of toluene = 200 mL;  $[Zr] = 2.5 \times 10^{-5}$  mol/L;  $[Al] = 0.025$  mol/L. <sup>b</sup> Refer to Table 1.

tions were performed at  $3.45 \times 10^3$  kPa and 130, 140, and 150 °C with a mean residence time of 4 min. The concentrations of CGC, TPF-PB, and MMAO were 15, 45, and 150  $\mu M$  for all runs. Table 1 shows the measured properties of the various macromonomers.

**Copolymerization Procedure.** The copolymerization reactions of propylene with EPR macromonomer were performed in our 0.5 L semibatch reactor (SBR). The details regarding the reactor system were reported in our previous work.<sup>21</sup> In all experiments, the soluble macromonomer was dissolved in toluene and charged into the reactor. MMAO was injected into the system, and 5 min later, the catalyst was introduced. The MMAO and catalyst concentrations in the reactor were 0.025 and  $2.5 \times 10^{-5}$  mol/L, respectively. The reactor was evacuated, and the polymerization was initiated by pressurizing with 12.5 psig propylene. The reaction was allowed to proceed for 30 min and was terminated by depressurizing and injecting 5 mL of methanol. The resultant polymer was filtered and washed three times with 60 °C toluene to remove any unreacted macromonomer. It was then washed with a 1% HCl methanol solution to remove MMAO residue, filtered, and dried in a vacuum oven. The toluene extract was collected, and the solvent evaporated. The unreacted macromonomer was dried for 72 h in a vacuum oven and was massed and analyzed. The detailed polymerization conditions are summarized in Table 2.

**Polymer Characterization.** Molecular weight (MW) and MWD of the polymers were measured using a Waters–Millipore 150 C high-temperature gel permeation chromatograph (GPC) with a differential refractive index (DRI) detector. The polymer samples were dissolved in 1,2,4-trichlorobenzene (TCB) at a concentration of 0.1 wt % and measured at 140 °C

**Table 3. Results of the Copolymerization of Propylene with Poly(ethylene-co-propylene) Macromonomers Using Semibatch Reactor**

copolym no. <sup>a</sup>	$M_n$ (kg/mol)	PDI	yield (g)	EPR conv <sup>b</sup> (%)	EPR conv <sup>c</sup> (%)	residual macrom $M_n$	wt % EPR	LCBF <sup>d</sup>	LCBF <sup>e</sup>	$\eta_0^*(\times 10^{-3})$ (Pa s)	$n$
1	59.0	2.7	13.1	25.0	25.4	3370	7.6	2.8 (1.8)	2.3	1.03	0.63
2	59.1	2.7	10.3	27.5	28.2	5100	10.7	2.4 (1.6)	2.2	1.05	0.62
3	54.8	2.6	14	30.0	30.8	7400	8.6	1.1 (0.8)	<i>f</i>	1.63	0.62
4	41.0	3.2	10.8	32.7	<i>f</i>	9780	15.7	1.1 (0.8)	<i>f</i>	2.32	0.58
5	41.0	2.9	9.3	30.0	<i>f</i>	14 340	16.1	0.9 (0.6)	<i>f</i>	3.03	0.56
6	99.0	2.8	6.9	17.1	<i>f</i>	21 720	8.7	1.0 (0.4)	<i>f</i>	24.5	0.42
7	97.7	2.5	9.5							10.4	0.60
8	53.0	2.7	16.5	40.0	<i>f</i>	<i>f</i>	2.4	(0.5)	<i>f</i>	0.76	0.61
9	55.2	2.4	15.7	35.0	34.8	<i>f</i>	4.5	(1.0)	<i>f</i>	0.68	0.63
10	48.3	2.7	15.6	28.3	<i>f</i>	<i>f</i>	5.4	(1.0)	<i>f</i>	0.86	0.62
11	75.0	2.4	13.8	20.0	<i>f</i>	<i>f</i>	1.4	(0.1)	<i>f</i>	1.35	0.58
12	80.0	2.3	15.3	25.0	<i>f</i>	<i>f</i>	3.3	(0.2)	0.25	4.72	0.52
13	31.7	2.4	22.5	30.0	31.3	3230	5.3	1.0 (0.7)	<i>f</i>	<i>f</i>	<i>f</i>
14	29.4	2.4	20.2	32.5	33.4	3180	4.5	0.9 (0.8)	<i>f</i>	<i>f</i>	<i>f</i>

<sup>a</sup> The copolymer sample number corresponds to the run number in Table 2. <sup>b</sup> Measured by massing unreacted macromonomer. <sup>c</sup> Determined using FTIR. <sup>d</sup> Determined by massing unreacted macromonomer and using it in eqs 3 and 4. In parentheses,  $M_n$ (macromonomer, original) used in eq 3 because of the unavailability of  $M_n$ (macromonomer, grafted). <sup>e</sup> Measured using  $^{13}\text{C}$  NMR. <sup>f</sup> Not measured.

with a flow rate of 1 mL/min. The GPC was equipped with three linear mixed Shodex AT806MS columns. The retention times were calibrated at 140 °C against monodisperse TSK polystyrene (PS) standards from TOYO SODA Mfg. Co. The Mark-Houwink constants for the universal calibration curve were  $K = 2.32 \times 10^{-4}$  and  $\alpha = 0.653$  for PS,  $K = 3.95 \times 10^{-4}$  and  $\alpha = 0.726$  for PE, and  $K = 1.54 \times 10^{-4}$  and  $\alpha = 0.760$  for PP.

$^{13}\text{C}$  NMR spectra were acquired on a Bruker AC 300 pulsed NMR spectrometer operated at 75.4 MHz with broad band decoupling. The samples were dissolved in deuterated *o*-dichlorobenzene (*d*-ODCB) and TCB and were measured at 120 °C using 10-mm sample tubes. *d*-ODCB was used to provide an internal lock signal, and TCB was the internal reference. Spectra required more than 7000 scans to attain an acceptable signal-to-noise ratio. A repetition time of 10 s was utilized.<sup>22</sup>

The vinyl and vinylidene concentrations of the macromonomer were measured using an IR spectrometer according to ASTM D 3124-93 and ASTM D 5576-94 procedures.<sup>23,24</sup> The samples were prepared in KBr cells with a thickness of 0.1 mm. Standard solutions were prepared using 1-octene and heptane.

All rheological measurements were conducted on a Stresstech HR parallel-plate rheometer in dynamic mode with a gap of 1.5 mm. Samples were measured in 10 °C increments between the temperatures of 170 and 220 °C under a nitrogen blanket to prevent degradation. Strain sweeps were performed prior to frequency sweeps to establish the linear region. A frequency range of  $10^{-2}$  to 65  $\text{s}^{-1}$  was investigated using a variable strain method. This method entails using the maximum strain that is within the linear region. The test samples were first treated with 0.6 wt % antioxidant and were compression-molded (20 mm diameter and 2 mm thickness) at 160 °C and 2 MPa for 6 min followed by rapid quenching.

## Results and Discussion

**Sample Characterization.** Table 3 summarizes the high-temperature gel permeation chromatography (GPC),  $^{13}\text{C}$  NMR, FTIR, and parallel-plate rheometry characterization results.

The incorporation of EPR macromonomers onto growing PP chains was verified using several techniques. First, the unreacted macromonomer was extracted from the copolymer using toluene at 60 °C. The toluene was removed, and the remaining macromonomer was dried and massed. This gave a direct estimate for the amount of macromonomer grafted in the copolymer.

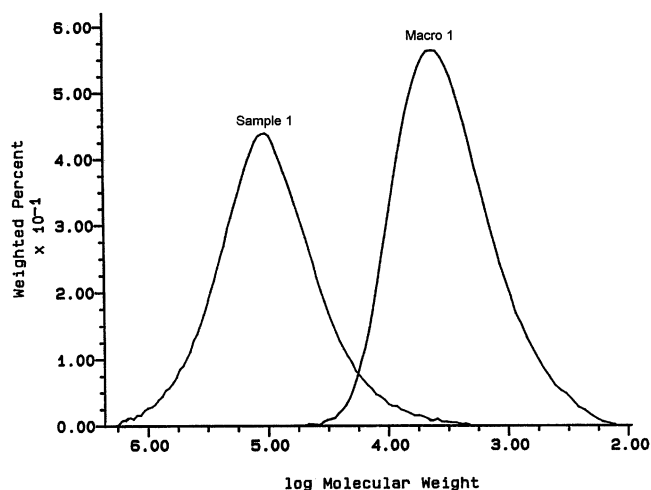


**Figure 1.** GPC trace of sample 1 overlaid with the trace of macromonomer.

Further analysis revealed that the separation of unreacted macromonomer from copolymer using hot solvent extraction was extremely effective. There were no discernible peaks where unreacted macromonomer would elute, indicating that there was no significant amount of residual macromonomer in the copolymer. Figure 1 shows a representative GPC trace of sample 1 overlaid with the trace of unreacted macromonomer.

An end group analysis using FTIR spectroscopy was performed to further verify the grafting reaction and to determine the extent of this reaction. The macromonomers were first analyzed to determine the concentration and type of end groups. The peaks were assigned using the method outlined in ASTM D 3124-93 and ASTM D 5576-94.<sup>14,15</sup> The two peaks observed at 887 and 910  $\text{cm}^{-1}$  were attributed to vinylidene and vinyl end groups, respectively. It was found that the EPR macromonomer was composed of approximately 80% unsaturated end groups with similar concentrations of vinyl and vinylidene, as shown in Table 1.

Subsequently, several unreacted macromonomer samples were examined to determine the conversion of these end groups. This analysis revealed that the incorporation of macromonomer was efficient, having vinyl conversions of 70–90%. Further inspection also showed that only vinyl end groups were incorporated

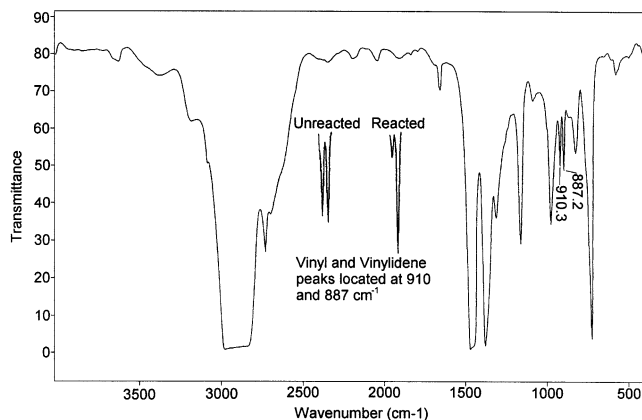


**Figure 2.** FTIR spectrum of sample 3 macromonomer before and after copolymerization.

into growing polymer chains. Macromonomer with terminal vinylidene did not participate in the copolymerization. These results match the conversions determined by massing the unreacted macromonomer, as seen in Table 3. Figure 2 shows the FTIR plots of the macromonomer used in sample 3, before and after polymerization.

Further analysis using the MWs of the EPR and the copolymer, determined by GPC, allowed the calculation of the long chain branch frequencies using

$$\text{LCBF} = \frac{\frac{\text{mass}(\text{macrom,grafted})}{M_n(\text{macrom,grafted})}}{\frac{\text{mass}(\text{copolymer})}{M_n(\text{copolymer})}} \quad (3)$$

A comparison of molecular weights was also conducted on the original and residual macromonomers. In all cases, the residual macromonomer had a significantly higher molecular weight than the original. The original macromonomer used in run 1 had a  $M_n$  of 2560 g/mol. After reacting, the residual macromonomer had a  $M_n$  of 3370 g/mol. Similarly, macrom 2 (in run 2) increased from 3900 to 5100 g/mol and macrom 3 (in run 3) increased from 6010 to 7400 g/mol after reacting. These data indicate that the copolymerization is dependent on the macromonomer MW with shorter chains preferentially reacted. This MW-dependent behavior was also observed in a systematic study of increasing macromonomer MW shown in a later section.

The MW of the grafted macromonomer could not be measured directly. However, it could be estimated from the measured MWs of the original and residual samples,

$$\frac{\text{mass}(\text{macrom,grafted})}{M_n(\text{macrom,grafted})} = \frac{\text{mass}(\text{macrom,original})}{M_n(\text{macrom,original})} - \frac{\text{mass}(\text{macrom,residue})}{M_n(\text{macrom,residue})} \quad (4)$$

The  $M_n$  of the residual macromonomer was not available for all of the runs. For these samples, the original  $M_n$  was used in eq 3 for the LCBF estimation.

The LCBF values estimated from eqs 3 and 4 were then verified using  $^{13}\text{C}$  NMR with peaks assigned using the method outlined by Shiono et al.<sup>14</sup> Figure 3 shows the  $^{13}\text{C}$  NMR spectra of sample 12. The strong resonances of methylene, methine, and methyl carbons of

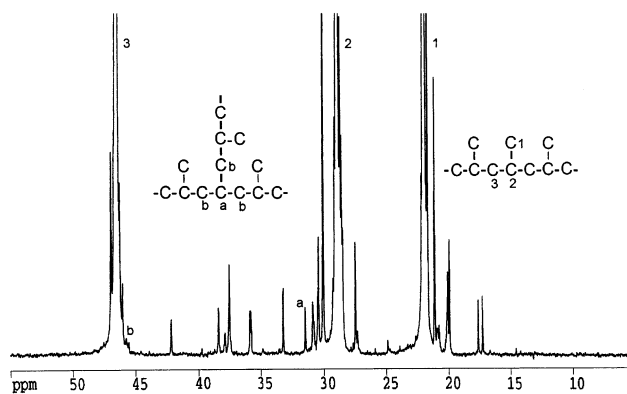


**Figure 3.**  $^{13}\text{C}$  NMR spectrum of sample 12.

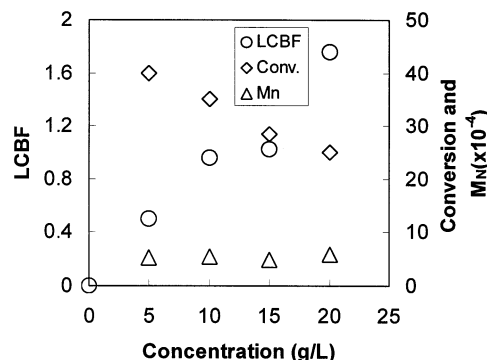


**Figure 4.** Influence of low MW macromonomer concentration on LCBF, copolymer  $M_n$ , and conversion.

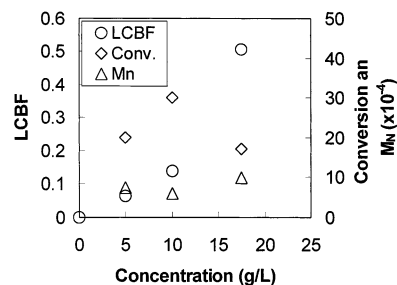


**Figure 5.** Influence of high MW macromonomer concentration on LCBF, copolymer  $M_n$ , and conversion.

the PP backbone are observed at around 46, 28, and 21 ppm. The peak associated with the conjunction carbon of iPP backbone with EPR side chain was assigned a chemical shift of 31.7. The intensity of this peak was used to determine the level of long chain branching. Three samples were measured with  $^{13}\text{C}$  NMR, and the values shown in Table 3 were found to be in agreement with those calculated using massed, unreacted macromonomer.

**Effect of Macromonomer Concentration on the Copolymerization.** The influences of the initial concentration of macromonomer on the molecular weight and LCBF of the copolymer, as well as the conversion of macromonomer, were studied. Two different macromonomers were used, one well below the critical entanglement length (runs 8, 9, 10, and 1 using macrom 1) and the other well above (runs 11, 12, and 6 using macrom 6). The initial concentration was varied from 0 to 20 g/L. Figures 4 and 5 show the influence of macromonomer concentration on the conversion, molecular weight of copolymer, and incorporation of macromonomer for both series. It was found that when macrom 1 was copolymerized, the initial concentration

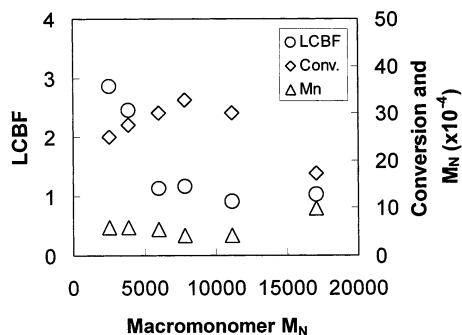


**Figure 6.** Influence of macromonomer MW on LCBF, copolymer  $M_n$ , and conversion.

had little influence on the molecular weight of the resultant copolymer. The  $M_n$  remained approximately constant at about 54 000 g/mol. Varying the charge of EPR from 5 to 20 g/L had a strong influence on the LCBF. The LCBF changed from 0.5 to 2.8 branches per chain. Controlling the stoichiometry of the macromonomer provided an effective method for controlling the branch density while maintaining a constant molecular weight copolymer. It can also be seen that increasing the initial charge of macromonomer decreased the conversion. The conversion varied from 40% to 25% when the macromonomer charge was increased from 5 to 20 g/mol. When macrom 6 was copolymerized, however, the initial concentration influenced both LCBF and  $M_n$ . Increasing the initial charge of macrom 6 from 5.0 to 17.5 g/L increased the LCBF from 0.1 to 0.4 branches per chain. It also increased the  $M_n$  from 75 000 to 99 000 g/mol. Further, the conversions of macrom 6 were approximately at 20–30%, lower than those of macrom 1.

**Effect of Macromonomer Molecular Weight on the Copolymerization.** The influences of the macromonomer molecular weight on the copolymer molecular weight and LCBF, as well as the macromonomer conversion, were studied. The macromonomer  $M_n$  was varied from 2500 to 17 000 g/mol. Figure 6 shows the LCBF, copolymer MW, and macromonomer conversion versus the macromonomer  $M_n$ . An effort was made to prepare a series of long chain branched samples having similar LCBFs while varying the branch  $M_n$  for rheological characterization purposes. This was attempted by varying the initial charge of macromonomer in the reaction. The macromonomer charge was increased from 20 g/L in runs 1–3 to about 25 g/L in runs 4 and 5 (see Table 2). However, the charge in run 6 was reduced to 17.5 g/L because of solubility limitations of the high molecular weight macromonomer. Except for the run 1 and run 2 samples, the others had the LCBFs approximately equal to 1. The charge of macrom 1 was lowered from 20 to 10 g/L (run 9) to prepare the low molecular weight side chain sample having the LCBF about 1.0.

At the same macromonomer charge, increasing the macromonomer  $M_n$  decreased the LCBF, particularly at the low  $M_n$  range. It is more difficult for the higher  $M_n$  macromonomer chains to be incorporated into the growing polypropylene backbones because of chain translational diffusion limitations or trapping of terminal vinyl groups in large chain coils or both. The conversion versus macromonomer  $M_n$  curve showed a maximum. The conversion initially increased with increasing macromonomer  $M_n$ . When the  $M_n$  exceeded 7800 g/mol, the conversion started to decrease. The

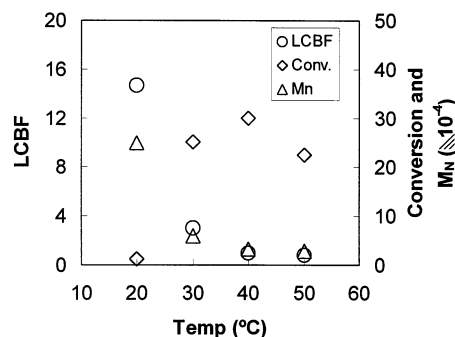


**Figure 7.** Influence of reaction temperature on LCBF, copolymer  $M_n$ , and conversion.

conversion depended on the molar concentration of charged macromonomer. It was also affected by the chain-length-dependent incorporation. Lowering the molar concentration of macromonomer would lead to a higher conversion. The weight charges in runs 1, 2, and 3 were the same at 20 g/L. However, the molar content of run 1 was the highest, followed by run 2 and run 3, because of their different  $M_n$ 's, resulting in the higher conversion in run 3 than that in run 2 and run 1. The conversion decrease in the high macromonomer  $M_n$  range was mainly caused by the chain-length-dependent incorporation. The copolymer molecular weights remained relatively constant, except for run 6, which had significantly higher  $M_n$ .

**Effect of Polymerization Temperature on the Copolymerization.** The polymerization temperature was varied to study its influence on the macromonomer reactivity. Figure 7 shows the effect of temperature on the LCBF, copolymer MW, and macromonomer conversion. It was observed that the macromonomer conversion increased with increasing temperature. However, the reactivity of propylene also greatly increased. There was significantly more sample produced. Despite the increase in the mass of incorporated macromonomer, the ratio of macromonomer to propylene in the copolymer actually decreased, leading to lower LCBFs. As was also expected, the temperature had a strong influence on the molecular weight of the resultant copolymers, producing significantly higher MWs at low temperatures.

**Rheological Responses.** The influences of long chain branch length and frequency on the storage modulus,  $G'(\omega)$ , loss modulus,  $G''(\omega)$ , and complex viscosity,  $\eta^*$ , as defined in eq 5, were investigated.

$$\eta^* = \left[ \left( \frac{G'}{\omega} \right)^2 + \left( \frac{G''}{\omega} \right)^2 \right]^{1/2} \quad (5)$$

The rheological data, generated at multiple temperatures, was superimposed to 190 °C using the shift factor  $a_T$  given in eq 1. The activation energies were calculated using low shear viscosities as shown in eq 2.

The long chain branched samples had very long relaxation times at low shear rates, and it was not possible to obtain frequency-independent viscosities from which the Newtonian viscosities ( $\eta_0$ ) could be inferred. An attempt at fitting the viscosity data using the Cross equation, given by eq 6, was made.<sup>27</sup>

$$\eta^*(\omega) = \frac{\eta_0}{[1 + (\lambda\omega)^n]} \quad (6)$$

where the value of  $n$  was assumed to be independent of temperature and the characteristic time,  $\lambda$ , to be pro-

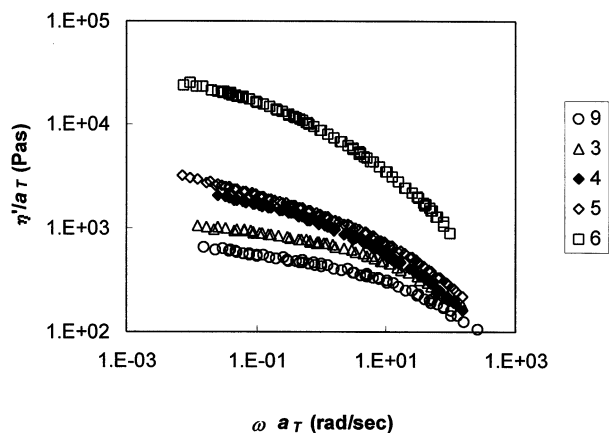


**Figure 8.** Influence of branch MW on the dynamic viscosity.

portional to  $\eta_0$ . Unfortunately, solutions were not found for these samples. Therefore, we have approximated  $\eta_0$  with the complex viscosity measured at  $\omega = 0.01 \text{ s}^{-1}$ . To quantify the shear-thinning behavior, the power-law expression, given by eq 7, was fitted to the viscosity data at high shear rates.

$$\eta^* = m\omega^{n-1} \quad (7)$$

where  $m$  is the consistency and  $n$  is the power-law exponent, which indicates the degree of non-Newtonian behavior.

**Effect of Macromonomer Molecular Weight on the Rheology.** The influences of the long chain branch MW on the  $\eta^*$ ,  $G'$ ,  $G''$ , and apparent  $E_a$  were studied. The MW, MWD, and LCBF of samples 3, 4, 5, 6, and 9, as shown in Table 3, were determined to be similar, with the exception of sample 6. Therefore, we feel justified in comparing the rheological responses of these samples. Figure 8 shows the complex viscosities of the samples with various branch lengths, ranging from well below  $M_c$  to well above.

From this figure, it is readily apparent that the branch length had a significant influence on the complex viscosity over the entire frequency range studied. Sample 9, with long chain branch lengths below  $M_c$ , behaved similarly to linear PP. The EPR branches were not long enough to form sufficient entanglements to affect the viscosity. When the branch  $M_n$  was increased to 6000 g/mol, a significant enhancement in  $\eta_0^*$  was seen. Further increases in the branch  $M_n$  led to greater increases in  $\eta_0^*$ . At low shear rates, the viscosity is dominated by the relaxation behavior of branched polymer molecules. An increase in branch  $M_n$  permits the formation of additional entanglements, leading to increased low shear viscosities.

It must be noted that there was a significant decrease in the copolymer  $M_n$  from sample 3 (54.8 kg/mol) to sample 4 (41.0 kg/mol). Despite this decrease, the viscosity of sample 4 was markedly higher. At high shear rates, the viscosity is dominated by the reptation of linear chains. Consequently, because these samples had similar  $M_n$ , it was expected that the high shear viscosities would be similar. This behavior was indeed observed in Figure 8. When the shear rate approached  $100 \text{ s}^{-1}$ , the viscosities almost overlapped. This phenomenon also had a significant influence on the shear thinning of the polymer samples.

Figure 9 shows a plot of the power-law exponent  $n$  and the low shear viscosity measured at  $190^\circ\text{C}$  versus

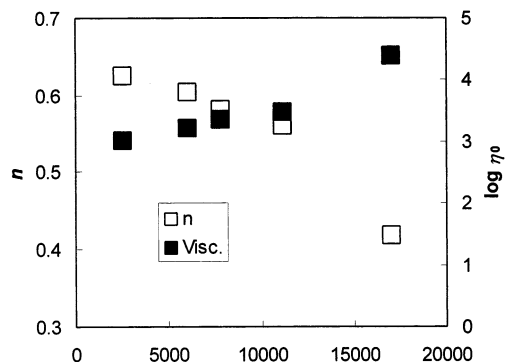


**Figure 9.** Influence of branch length on the power-law exponent  $n$  and on the  $\eta_0^*$ .

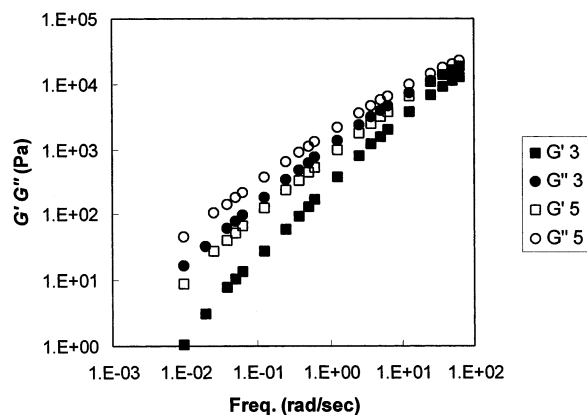


**Figure 10.** Influence of branch length on  $G'$  and  $G''$ .

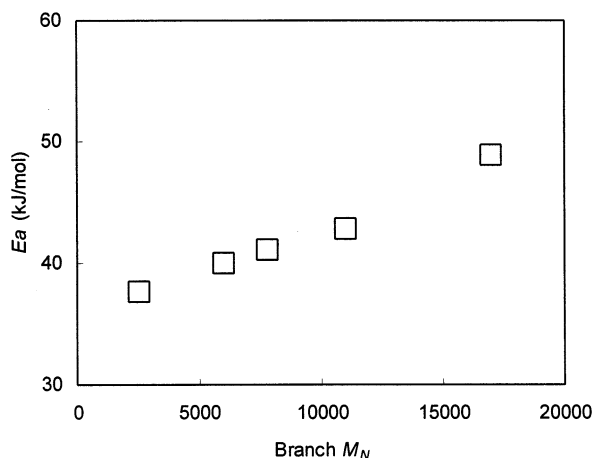


**Figure 11.** Influence of branch length on activation energy.

branch length. It can be seen that increasing the branch  $M_n$  significantly increased the shear-thinning behavior of the copolymers. The power-law exponent  $n$  shows a rapid decrease with increasing branch length, indicating a further deviance from Newtonian behavior.

The branch length also had a significant influence on the loss and storage moduli. The values of  $G'$  and  $G''$  for samples 3 and 5 at  $170^\circ\text{C}$  are shown in Figure 10 with the remainders omitted to prevent crowding. Samples 3 and 5 had similar MWs and MWDs with branch  $M_n$  of 6000 and 11 100, respectively. It is readily apparent that sample 5, with a longer branch length, had significantly higher values of  $G'$  and  $G''$  at low shear rates, while at high shear rates, they were similar.

The branch MW had a significant influence on the flow activation energy, as can be seen in Figure 11.

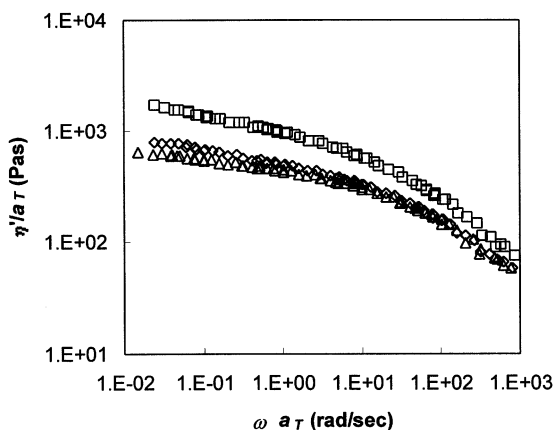


**Figure 12.** Influence of LCBF on dynamic viscosity having branches of  $M_n = 2500$  g/mol.

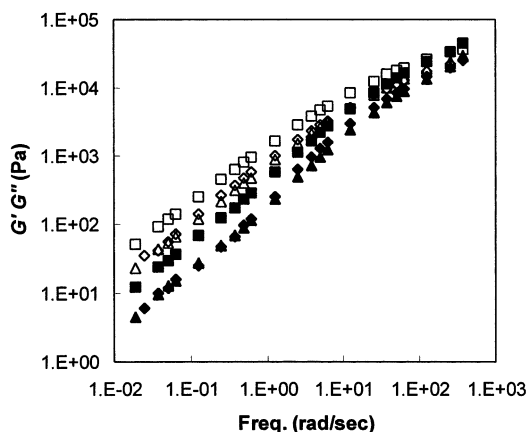


**Figure 13.** Influence of LCBF on  $G'$  and  $G''$  with branches of  $M_n = 2500$  g/mol.

When the branch  $M_n$  was 2500 g/mol, the observed activation energy was 37.7 kJ/mol. This is only slightly above the accepted value for linear PP.<sup>25</sup> As the branch length was increased, the  $E_a$  increased linearly to a maximum of 48.9 kJ/mol at a branch  $M_n$  of 17 000. This value is significantly higher than that of linear PP but still lower than the 55 kJ/mol reported by Kurzbeck et al.<sup>26</sup> for PP modified with electron-beam irradiation.

**Effect of LCBF on the Rheology.** To verify the influence of long chain branching beneath the critical entanglement length, the LCBF was varied from 0.5 to 1.8 with a branch  $M_n$  of 2500 g/mol. The MW and MWD of these samples were similar with  $M_n$  of approximately 55 000 g/mol. Figure 12 shows a plot of  $\eta^*$  versus frequency for samples 8, 9, and 1. From this figure, it is readily apparent that the LCBF did not have a significant influence on the  $\eta^*$  when the branch length was 2500 g/mol. It is theorized that the EPR branches were not long enough to form entanglements and consequently behaved as short chain branches. Figure 13, meanwhile, shows  $G'$  and  $G''$  versus frequency. Again, the LCBF had minor influence on the loss and storage moduli when the branch  $M_n$  was 2500 g/mol. It was also shown, in Figure 14, that when the branch  $M_n$  was 2500 g/mol, the LCBF had no significant influence on  $E_a$ .

The influence of the frequency of long chain branches with MWs above  $M_c$  was also studied. Figure 15 shows a plot of  $\eta^*$  versus frequency for samples 11, 12, and 6, which have a branch  $M_n$  of 17 000 g/mol. These samples have copolymer  $M_n$  ranging from 60 000 to 99 000 g/mol,

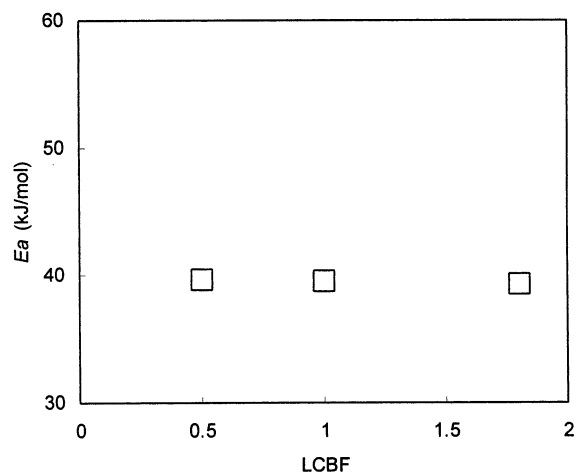


**Figure 14.** Influence of LCBF on  $E_a$  with branches of  $M_n = 2500$  g/mol.

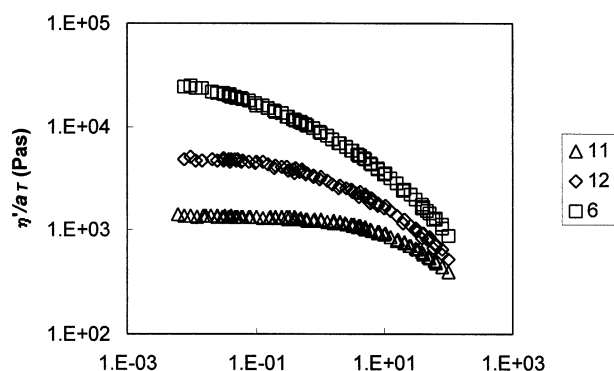
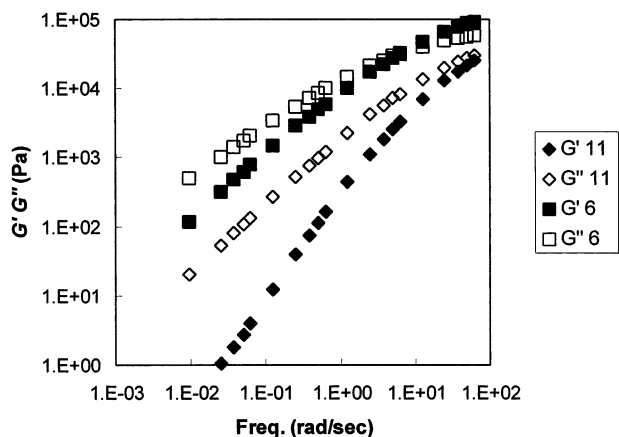


**Figure 15.** Influence of LCBF on dynamic viscosity with branches of  $M_n = 17\,000$  g/mol.

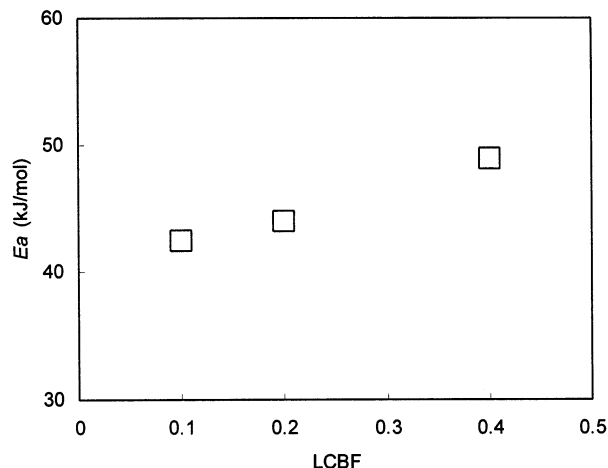
and consequently, the MW may have had an influence on the observed rheological responses. It can readily be seen that the LCBF had a significant affect on the  $\eta^*$  over the entire frequency range. As was expected, the  $\eta_0^*$  was a sensitive indicator of branch frequency, significant enhancements being observed with increased LCBFs. The viscosity at low shear rates is dominated by the relaxation of branched molecules. An increase in the branching frequency increases the number of entanglements and leads to an enhancement in  $\eta_0^*$ . The LCBF also affected the shear-thinning phenomenon. Sample 6, with a LCBF of 0.4, exhibited considerably more shear thinning than sample 12 with a LCBF of 0.2. Sample 12 in turn was more shear-sensitive than sample 11 with a LCBF of 0.1.

Figure 16 shows the influence of LCBF on  $G'$  and  $G''$ . It is apparent that the LCBF had a strong influence on the dynamic moduli. Sample 6 had considerably higher values for both  $G'$  and  $G''$  than sample 11. Sample 6 also exhibited a broader relaxation spectrum as is evident by the more gradual increase in  $G'$ . This behavior is attributed to the additional modes of relaxation provided by long chain branching.

It is readily apparent in Figure 17 that the LCBF of samples with branch  $M_n$  of 17 000 had a significant influence on  $E_a$ . It was observed that  $E_a$  varied linearly with LCBF. It is interesting to compare the behavior observed in Figures 12–14 with that in Figures 15–17. When the MW of the branches was 2500 g/mol, which is below  $M_c$ , the long chain branch frequency did not appear to have a large influence on the measured rheological responses. However, when the branch length



**Figure 16.** Influence of LCBF on  $G'$  and  $G''$  with branches of  $M_n = 17\,000$  g/mol.



**Figure 17.** Influence of LCBF on  $E_a$  with branches of  $M_n = 17\,000$  g/mol.

was increased to 17 000 g/mol, the LCBF had a strong influence on  $\eta^*$ ,  $G'$ ,  $G''$ , and  $E_a$ .

**Thermorheological Complexity.** The long chain branched PP samples produced in this study were examined for the thermorheological complexity observed in LCB PE. The method outlined by Wood-Adams and Costeux<sup>18</sup> was used to determine rheological complexity. Plots of  $G^*$  versus  $\eta_0\omega$  are temperature-independent for simple materials and display temperature dependence for complex materials. On the basis of this criterion, only sample 6 exhibited rheological complexity as shown in Figure 18. The shift factor  $a_T$  was determined for the entire experimental frequency range for sample 6 using  $G'$ . Figure 19 shows the activation energy versus shear rate for samples 1 and 6. It can be seen that sample 1 exhibited simple rheological behavior while the activation energy of sample 6 showed a dependence on the shear rate. Sample 6 had an activation energy of approximately 50 kJ/mol at  $\omega = 0.01$  s<sup>-1</sup>, which is similar to the value calculated using  $\eta_0$ . At higher shear rates, the activation energy decreased to 29.2 kJ/mol. This behavior is attributed to the additional modes of relaxation at low shear rates caused by branched molecules. The rheological behavior at high shear rates is dominated by the reptation of linear chains. Therefore, the activation energy of sample 6 at high shear rates is similar to that of linear PP.

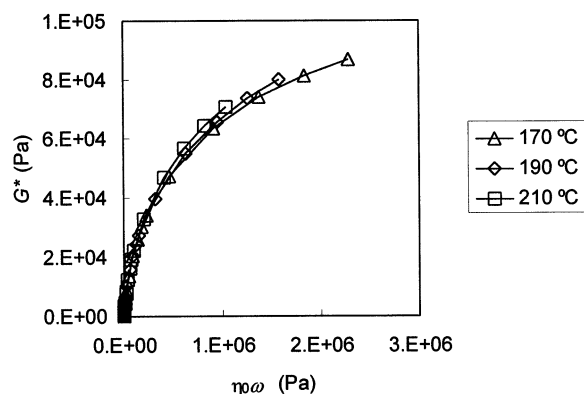


**Figure 18.** Rheological complexity of sample 6.

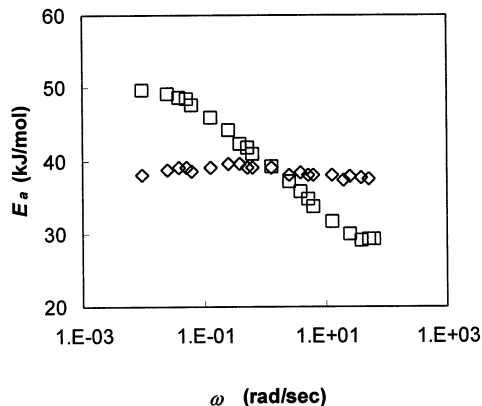


**Figure 19.** Time-dependent activation energies of samples 1 and 6.

## Conclusions

Propylene was copolymerized with poly(ethylene-*co*-propylene) (EPR) macromonomers in a semibatch polymerization using *rac*-dimethylsilylenebis(2-methylbenz-[e]indenyl) zirconium dichloride/modified methylaluminoxane. The resultant polymer was composed of an isotactic polypropylene backbone with EPR branching. It was found that the stoichiometry of the macromonomer could be used to efficiently control the long chain branch frequency (LCBF) of the copolymer without greatly influencing the molecular weight. It was also possible to control the long chain branch length by controlling the macromonomer  $M_n$  with the branch lengths ranging from 2500 to 17 000 g/mol.

The rheological behavior of the resultant long chain branched polypropylenes was also examined. It was shown that when the branch  $M_n$  was less than 7000 g/mol, it behaved as a short chain branch and had little influence on the rheological responses. When the branch  $M_n$  was greater than 7000 g/mol, it was long enough to form entanglements and behaved as a long chain branch. The branch length had a significant influence on the rheological responses. Both  $G'$  and  $G''$  showed elevated values at low shear rates. The  $\eta_0^*$  was a sensitive indicator of branch length. Increasing branch  $M_n$  led to enhanced values of  $\eta_0^*$ . The shear-thinning phenomenon also increased with increasing branch length, as did the flow activation energy. The long chain branch frequency also had a strong influence on the rheological behavior of the polymer samples provided the branch  $M_n$  was greater than 7000 g/mol. The increase in LCBF led to increased  $\eta_0^*$ , increased shear thinning, enhanced flow activation energy, and elevated

values of  $G'$  and  $G''$ . The long chain branched samples were found to exhibit thermorheologically simple behavior, except for sample 6.

**Acknowledgment.** The authors thank the Ministry of Education, Science and Technology of Ontario for the PREA support for the work. We also thank the Canada Foundation of Innovation (CFI) for the supports for research facilities.

## References and Notes

- (1) Carella, J. M.; Gotro, J. T.; Graessley, W. W. *Macromolecules* **1986**, *19*, 659.
- (2) Small, P. A. *Adv. Polym. Sci.* **1975**, *18*, 1.
- (3) Santamaria, A. *Mater. Chem. Phys.* **1985**, *12*, 1.
- (4) Carella, J. M.; Gotro, J. T.; Graessley, W. W. *Macromolecules* **1986**, *19*, 659.
- (5) Milner, S. T.; McLeish, T. C. B.; Young, R. N.; Hakiki, A.; Johnson, J. M. *Macromolecules* **1998**, *31*, 9345.
- (6) Milner, S. T.; McLeish, T. C. B. *Macromolecules* **1998**, *31*, 7479.
- (7) Lohse, D. J.; Milner, S. T.; Fetters, L. J.; Xenidou, M.; Hadjichristidis, N.; Mendelson, R. A.; Garcia-Franco, C. A.; Lyon, M. K. *Macromolecules* **2002**, *35*, 3066.
- (8) Kaminsky, W. In *Transition Metal Catalyzed Polymerization*; Quirk, R. P., Ed.; MMI Press: London, 1983; pp 225.
- (9) Chien, J. C. W.; Wang, B. P. *J. Polym. Sci., Polym. Chem. Ed.* **1988**, *26*, 3089.
- (10) Yan, D.; Wang, W.-J.; Zhu, S. *Polymer* **1999**, *40*, 1737.
- (11) Lai, S. Y.; Wilson, J. R.; Knight, G. W.; Stevens, J. C.; Chum, P. W. S. (The Dow Chemical Co., invs.) U.S. Patent 5,272,236, 1993.
- (12) Soga, K.; Uozumi, T.; Nakamura, S.; Toneri, T.; Teranishi, T.; Sano, T.; Arai, T. *Macromol. Chem. Phys.* **1996**, *197*, 4237.
- (13) Shiono, T.; Moriki, Y.; Ikeda, T. *Macromol. Chem. Phys.* **1997**, *198*, 3229.
- (14) Shiono, T.; Azad, S. M.; Ikeda, T. *Macromolecules* **1999**, *32*, 5723.
- (15) Weng, W.; Markel, E.; Dekmezian, A. *Macromol. Rapid Commun.* **2001**, *22*, 1488.
- (16) Jordan, E. A.; Donald, A. M.; Fetters, L. J.; Klein, J. *ACS Polym. Prepr.* **1989**, *30*, 63.
- (17) Raju, V. R.; Rachapudy, H.; Graessley, W. W. *J. Polym. Sci., Polym. Phys. Ed.* **1979**, *17*, 1223.
- (18) Wood-Adams, P.; Costeux, S. *Macromolecules* **2001**, *34*, 6281.
- (19) Park, S.; Wang, W.-J.; Zhu, S. *Macromol. Chem. Phys.* **2000**, *201*, 2203.
- (20) Wang, W.-J.; Kolodka, E.; Zhu, S.; Hamielec, A. E. *J. Polym. Sci., Part A: Polym. Chem.* **1999**, *37*, 2249.
- (21) Kolodka, E.; Wang, W.-J.; Charpentier, P. A.; Zhu, S.; Hamielec, A. E. *Polymer* **2000**, *41*, 3985.
- (22) Wang, W.-J.; Yan, D.; Zhu, S.; Hamielec, A. E. *Macromolecules* **1998**, *31*, 8677.
- (23) *Test Method for Vinylidene Unsaturation in Polyethylene by Infrared Spectrophotometry*; ASTM D 3124-98; American Society for Testing and Materials: Baltimore, MD, 2001; Vol. 8.02.
- (24) *Standard Practice for Determination of Structural Features in Polyolefins and Polyolefin Copolymers by Infrared Spectrophotometry*; ASTM D 5576-00; American Society for Testing and Materials: Baltimore, MD, 2001; Vol. 8.03.
- (25) Sugimoto, M.; Masubuchi, Y.; Takimoto, J.; Koyama, K. *J. Polym. Sci., Part B: Polym. Phys.* **2001**, *39*, 2692.
- (26) Kurzbeck, S.; Oster, F.; Munstedt, H. *J. Rheol.* **1999**, *43*, 359.
- (27) Cross, M. M. *J. Colloid Sci.* **1965**, *20*, 417.

MA021171M